arXiv:cond-mat/0111502v1 [cond-mat.supr-con] 27 Nov 2001

Core Strings and Flux Spreading Near Pinning Centers

D. J. Priour Jr[1,2], H. A. Fertig[1]
[1] *Department of Physics and Astronomy, University of Kentucky, Lexington, KY40506-0055*
[2] *Center for Computational Sciences, University of Kentucky, Lexington, KY40506-0045*
(February 1, 2008)

At the nucleus of a superconducting vortex is a small, circular core region where superconductivity is destroyed. Like an atomic nucleus, this core may become deformed, and such distortions can have important consequences in non-equilibrium situations. Using Ginzburg-Landau theory, we have investigated this phenomenon for vortices in the presence of artificial defects. We show that when a vortex approaches the vicinity of a defect, an abrupt transition occurs in which the vortex core develops a "string" extending to the defect boundary, while simultaneously the supercurrents and associated magnetic flux spread out and engulf the defect. The energetics of stretching the string determines the pinning behavior of the vortex. Experimental consequences of these strings are discussed.

PACS numbers: 74.20.-z, 74.60.Ge, 74.76.-w, 68.55.Ln, 61.46.+w

One of the most important properties of superconductors is their ability to carry currents without dissipation, allowing them to generate large magnetic fields. Many superconductors allow fields to penetrate in bundles of quantized magnetic flux, with associated whirlpools of current known as vortices. When these vortices are mobile, they spoil the perfect conductivity that make superconductors so useful. The quest to increase the maximum dissipationless current J_c that a superconductor may carry has thus fueled intense study of vortex pinning.

In recent years, pinning environments of artificially fabricated nanoscale defect arrays have been developed in hopes of better understanding and improving the pinning properties of superconductors. Some of the earlier contributions have involved macroscopic measurements (e.g. J_c, magnetization) performed on periodic "antidot" arrays [1–3]. The antidot regions contain material which is rendered non-superconducting. Pinning behavior may be studied in these periodic systems using various imaging techniques [1,4–7].

Much of the theoretical work on vortex pinning has employed numerical studies to focus [8] on the behavior of large collections of vortices under the influence of a driving force (supercurrent). Such studies usually employ simplified pinning potentials, in part to make possible simulations of large numbers of vortices, but also because information about pinning potentials at the microscopic level is simply unavailable. A few studies [9,10] have focused on energy scales for pinning varying numbers of flux quanta to the defects, as well as defect-vortex potentials as derived from the London equation [11,12]. However, the latter approach does not allow for variation of the Cooper pair density, and in particular cannot correctly treat the vortex core. In the London approach, vortex cores are usually assumed to be rigid in shape, and interactions of vortices with their environments are determined by the core position as well as the distribution of currents [11,12]. Our results demonstrate that the vortex core in fact deforms dramatically near an artificial defect: when the vortex center is sufficiently close to the defect, a *string* of suppressed order parameter develops from the vortex position to the pinning center edge, while the currents and magnetic flux spread out over a large area (see Fig. 2 below). The pinning potential of the vortex turns out to be dominated by the string when it is present, as we discuss below.

Methods– Our calculations focus on two dimensional arrays of artificial pinning centers in the form of holes in a bulk superconductor. Our goal is to find the lowest energy state of the system for specified locations of a superconducting vortex; from this we can construct a pinning potential. The appropriate description of the superconducting state is in terms of Ginzburg-Landau theory, which focuses on a complex superconducting order parameter $\psi(\vec{r})$, for which $|\psi|^2$ is proportional to the local density of superconducting electrons. Unlike the London theory, Ginzburg-Landau theory is valid at scales as small as the coherence length, ξ. Written in terms of dimensionless variables, the Ginzburg-Landau energy functional is

$$E_{GL} = \int \left[\begin{array}{c} \left| \psi^* \left(\vec{\nabla}/i - \vec{A} \right) \psi \right|^2 - |\psi|^2 \\ + \frac{\kappa^2}{2} |\psi|^4 + B^2 \end{array} \right] d^3x. \qquad (1)$$

In Eq. 1, $\vec{A}$ is the vector potential, and the magnetic field $\vec{B}(\vec{r}) = \vec{\nabla} \times \vec{A}$. $\kappa \equiv \frac{\lambda}{\xi}$ is the Ginzburg parameter, the ratio of the magnetic penetration depth λ and the coherence length. In this work, we report on results obtained for $\kappa = 8$. This choice of κ is deep enough into the high κ limit that, apart from scale factors in E_{GL} and ψ, the results vary little as κ is increased.

To analyze the behavior of the vortex near the pinning center, we employ a mean field approach in which one minimizes E_{GL} for a fixed vortex location to find ψ, $\vec{A}$, and the current $\vec{J}$. Our strategy for calculating ψ and

$\vec{A}$ self-consistently involves first holding ψ fixed at some initial guess, and minimizing E_{GL} with respect to $\vec{A}$ and $\vec{B}$. Next, we fix $\vec{A}$ and $\vec{B}$ and minimize with respect to ψ. These steps are iterated until changes in the variables become negligible. We implement this self-consistent approach numerically by dividing the unit cell into a fine lattice of small unit cells. In this discrete scheme, $\psi(\vec{r})$ is replaced by ψ_{ij} with ij specifying a grid point on a square lattice, while $\vec{A}_{ij}$ and $\vec{J}_{ij}$ are defined on nearest-neighbor links between the grid points. Derivatives in Eq. 1 are replaced by the corresponding finite differences. The resulting theory is very similar to lattice gauge theories studied in particle physics. To model the defect array as accurately as possible, one desires a fine grid; we find that with a 128×128 mesh our results are well-converged with respect to the discretization.

To see how one minimizes E_{GL} under the constraint of a specified vortex location, it is useful to write the current $\vec{J}$ in terms of the order parameter ψ and the vector potential $\vec{A}$. By minimizing E_{GL} with respect to the vector potential and employing a Maxwell equation one has

$$\begin{aligned} \vec{J} &= \frac{1}{2}\left[\psi^* \left(\vec{\nabla}/i - \vec{A}\right)\psi + \psi\left(-\vec{\nabla}/i - \vec{A}\right)\psi^*\right] \\ &= |\psi|^2 \left(\vec{\nabla}\phi - \vec{A}\right). \end{aligned} \tag{2}$$

In Eq. 2, we have used for the order parameter $\psi = |\psi| e^{i\phi}$. The familiar fluxoid quantization condition [13] arises from the requirement that the order parameter be single valued, i.e. $\oint \vec{\nabla}\phi \cdot d\vec{s} = 2\pi n_v$. Hence, in terms of $\vec{J}$ and $\vec{A}$,

$$\begin{aligned} 2\pi n_v(ij) &= \oint \left(\vec{J}/|\psi|^2\right) \cdot d\vec{s} + \oint \vec{A} \cdot d\vec{s} \\ &= \oint \left(\vec{J}/|\psi|^2\right) \cdot d\vec{s} + \Phi_B \end{aligned} \tag{3}$$

In the second part of Eq. 3, Φ_B is the total magnetic flux passing through the area of the contour, which we conveniently choose to be the small unit cell associated with the grid point ij, while $n_v(ij)$ is the total number of "fluxoid quanta" contained in the contour of integration [13]. It is through n_v that the vortex location(s) in the full unit cell of the system may be fixed: $n_v = 0$ except at the grid points where we wish to place a vortex, for which $n_v = 1$. Armed with knowledge of $|\psi|$ and some specified realization of $n_v(ij)$, one can solve for $\vec{J}$ and $\vec{A}$ via Eq. 3. Using the expression for the current given in Eq. 2, one obtains $\vec{\nabla}\phi$; inserting $\vec{\nabla}\phi$ and $\vec{A}$ into Eq. 1 yields an expression depending only on $|\psi|$ and κ which we minimize with respect to $|\psi|$ to obtain the order parameter modulus.

We note that the above method can be generalized to the case of a thin film superconductor. We have performed some calculations for such systems, and find that for antidot systems the results obtained are quite similar to the large κ results we report here. This may be understood in terms of the effective magnetic penetration depth for a thin film, $\lambda_{eff} = \frac{\lambda^2}{d}$, which is typically much larger than the bulk value λ [14]. This means that the energy stored in the magnetic field generated by the supercurrents is quite small, so that the fact that the field varies as one moves out of the plane has little impact on the state of the system. The resulting energy functional is thus nearly identical to the bulk three dimensional case, with columnar antidots and vortices.

Results– At large vortex-defect separations, the core has the usual compact structure with supercurrents localized about it. Fig. 1 presents a perspective plot of $|\psi|$, as well as a vector plot of the currents. The distances shown are in units of the coherence length, ξ. Our choice of a unit cell with side spanning 20 coherence lengths is typical of many of the nanoscale arrays studied experimentally. As the flux quantum nears the defect edge, it eventually reaches a critical distance d_c (typically several ξ, with precise value depending on the dot size and shape), where there is a sudden dramatic change. Fig. 2 illustrates the situation after the transition: the vortex core has developed a *string* extending from the flux quantum position to the defect edge; simultaneously the current now encircles the vortex-defect pair, and the magnetic flux created by these currents spreads over a larger area. The string is energetically favorable because it allows the formerly dense current of the vortex to spread out (engulfing the defect in the process), thereby reducing the kinetic energy of the state.

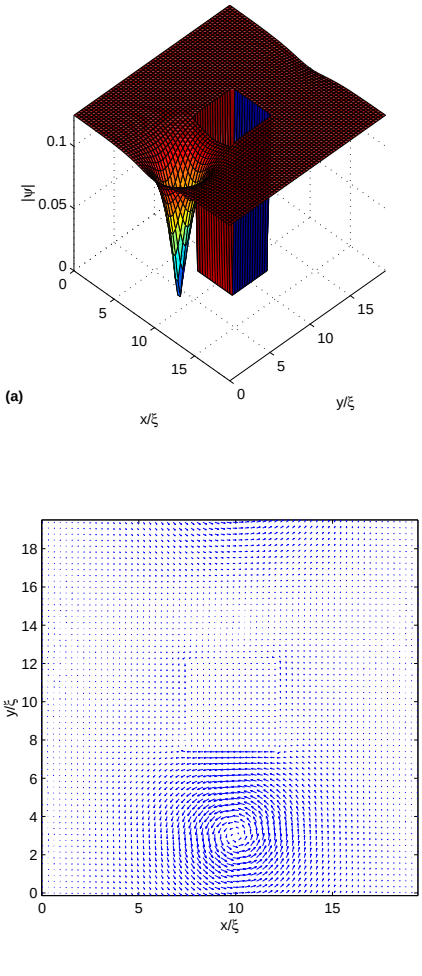

FIG. 1. A perspective plot of the order parameter modulus, $|\psi|$ (a) and current image (b) just prior to the transition. Currents are localized about the vortex core, which has a compact structure.

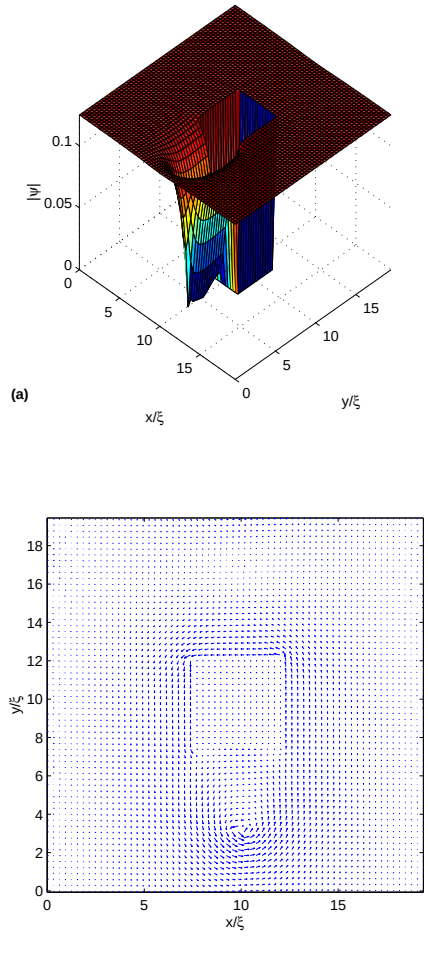

FIG. 2. Order parameter perspective plot (a) and currents (b) just after the transition. The currents circulate about the vortex-defect pair, and the vortex core has a string extending all the way to the defect edge.

When a net supercurrent flows across a superconductor, a Lorentz force is exerted on vortices; if these move in response energy is dissipated. In an artificial defect array, the driving force can be balanced by a pinning force given by the gradient of E_{GL} with respect to the vortex position. Hence, it is appropriate to regard E_{GL} as the pinning potential. Fig. 3 shows this as a function of distance from the unit cell edge, and it can be seen to have three distinct regions. For large separations, where the vortex core is compact, the pinning potential decreases relatively slowly. As the separation decreases it eventually crosses d_c and the core-string structure appears. Hysteresis in the calculations, indicated with arrows, suggests that the transition is first order. Below the transition one observes nearly linear behavior of the pinning potential, suggesting that the string carries an energy proportional to its length. The third region is announced by a discontinuous jump as the vortex is ab-

sorbed by the defect, followed by a perfectly flat region inside the defect. This abrupt jump is due to a sudden transformation of the order parameter. Immediately prior to absorption, constant Cooper pair density contours near the flux quantum have a semicircular profile. As the vortex enters the defect, this "semi-vortex" vanishes, removing a finite amount of energy for an infinitesimal change in the vortex position.

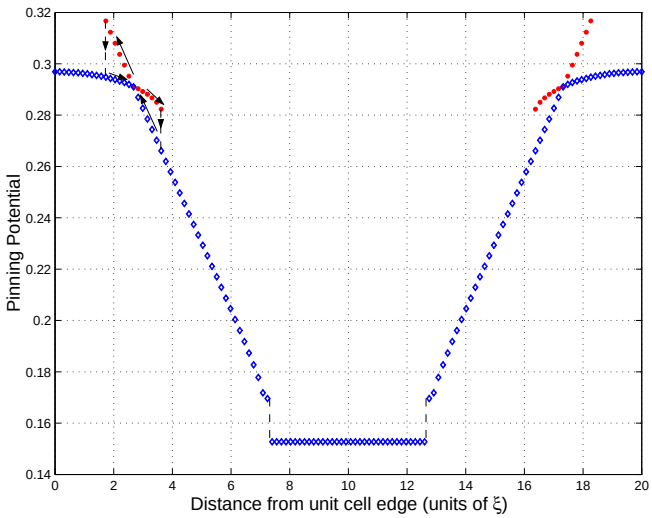

FIG. 3. Plot of the pinning potential showing broad linear regions and a gap in the potential at the defect boundary. The horizontal axis measures the distance of the vortex from the edge of the unit cell. Arrows and red circles indicate hysteresis in the calculation, a hallmark of a first order transition.

Experimental implications– The profile of the pinning potential shown in Fig. 3 suggests a set of measurements one might perform to seek an experimental signature of the unique pinning phenomena discussed above. One possible test would involve an AC driving current of magnitude small enough to leave the vortices pinned by the strings. Such a current would allow the vortices to "rattle around" in the linear part of the pinning well illustrated in Fig. 3 and produce losses, whereas a DC current of equal magnitude would be dissipationless. Upon lowering of the temperature the vortices would be captured by defects, leading to lossless supercurrents for both AC and DC driving forces. An observation of these effects would yield indirect confirmation of the form of the pinning potential we find. Something like this may recently have been observed [15]. Another interesting possibility is that a unique thermal depinning may occur as the temperature is increased in the regime of linear pinning. The presence of a string suggests that this may carry entropy at finite temperature, much as is the case of polymers. This entropy is proportional to the string length and temperature, and at high enough temperatures may overwhelm the energy per unit length found in our mean-field calculations. In analogy with polymer behavior [16], this leads to unbounded growth of the string and effective depinning of the vortex. However, it is not clear whether the string remains sufficiently well-defined at the temperatures necessary for proliferation that the polymer analogy remains valid up to the transition. Further research into this possibility is currently underway.

Ultimately the best confirmation of our results would involve imaging of the string. An interesting possibility in this context is to fabricate arrays with *two* defects per unit cell in close proximity. When one magnetic flux quantum passes through each unit cell, we have found solutions in which a string develops between the defects. Fig. 4 is an image of $|\psi|$ for an equilibrium configuration in a typical case. The existence of a string between defects opens the possibility of detecting these objects at low temperatures and without driving currents, simplifying the relevant experimental conditions.

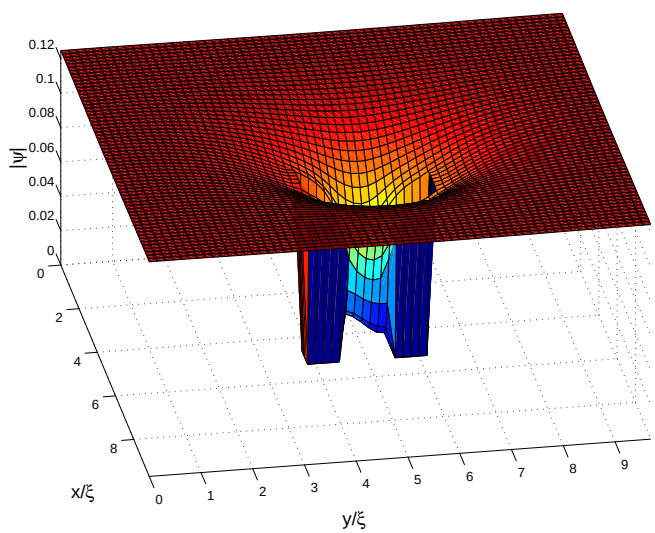

FIG. 4. Image of $|\psi|$ depicting a string connecting two defects in an experimentally realizable situation.

Summary– In the context of the Ginzburg-Landau theory, we have given a detailed treatment of the microscopic aspects of pinning phenomena in nanoscale periodic arrays. Strikingly, we see an apparent first order transition involving the creation of a string connecting the vortices to the defect, and an accompanying abrupt transformation of the supercurrent and the magnetic field it generates. The string configuration leads to a region of linear pinning. Absorption of the vortex by the antidot is marked by a jump in the pinning potential. Various aspects of the pinning potential should be observable in experiment.

Acknowledgments– The authors would like to thank L. E. DeLong, S. B. Field, and J. B. Ketterson for useful

discussions. This work was supported by NSF Grant No. DMR-9870681 and DMR-0108451.

---

[1] K. Harada et al. Science **274**, 1167 (1996).
[2] M. Baert, V. V. Metlushko, R. Jonckheere, V. V. Moshchalkov, and Y. Bruynseraede. Phys. Rev. Lett. **74**, 3269 (1995).
[3] V. V. Moshchalkov et al, Phys. Rev. B **54**, 7385 (1996).
[4] A. Tonomura et al, Nature **397**, 308-309, (1999)
[5] A. Tonomura et al, Nature **412**, 620-622, (2001)
[6] S. B. Field et al, cond-mat/0003415.
[7] T. Matsuda, K. Harada, H. Kasai, O. Kamimura, and A. Tonomura, Science **271**, 1393 (1996).
[8] F. Nori, Science **271**, 1373 (1996); C. Reichhardt, C. J. Olson, and F. Nori, Phys. Rev. Lett. 78, 2648-2651 (1997); M.C. Cha and H.A. Fertig, Phys. Rev. Lett. **80**, 3851 (1998).
[9] A. I. Buzdin, Phys. Rev B **47**, 11416 (1993).
[10] G. S. Mkrtchyan and V. V. Shmidt, Sov. Phys. JETP **34**, 195 (1972).
[11] I. B. Khalfin and B. Ya. Shapiro, Physica C **207**, 359 (1993).
[12] Sa-Lin Cheng, D.J. Priour Jr, and H.A. Fertig, cond-mat/0105601 (to be published in PRB).
[13] M. Tinkham, *Introduction to Superconductivity, Second edition*, McGraw-Hill, Inc., New York, (1996).,
[14] J. Pearl, Appl. Phys. Lett. **5**, 65 (1964); P.G. de Gennes, *Superconductivity of Metals and Alloys* Addison-Wesley, New York, (1989).
[15] J. Zhang, L.E. De Long, V. Majidi, and R.C. Budhani, Phys. Rev B **53**, R8851 (1996).
[16] C. Vanderzande, *Lattice Models of Polymers*, Cambridge University Press, Cambridge (1998).